Atmospheric
Chemistry
and Physics

NO$_3$ chemistry of wildfire emissions: a kinetic study of the gas-phase reactions of furans with the NO$_3$ radical

Mike J. Newland[1], Yangang Ren[1,a,b], Max R. McGillen[1], Lisa Michelat[1], Véronique Daële[1], and Abdelwahid Mellouki[1]

[1]ICARE-CNRS, 1C, avenue de la Recherche Scientifique, 45071 Orléans CEDEX 2, France
[a]now at: Research Center for Eco-Environmental Sciences, Chinese Academy of Sciences, Beijing 100085, China
[b]now at: University of Chinese Academy of Sciences, Beijing 100049, China

Correspondence: Mike J. Newland (mike.newland@cnrs-orleans.fr) and Abdelwahid Mellouki (mellouki@cnrs-orleans.fr)

Abstract. Furans are emitted to the atmosphere during biomass burning from the pyrolysis of cellulose. They are one of the major contributing volatile organic compound (VOC) classes to OH and NO$_3$ reactivity in biomass burning plumes. The major removal process of furans from the atmosphere at night is reaction with the nitrate radical, NO$_3$. Here, we report a series of relative rate experiments in the 7300 L indoor simulation chamber at Institut de Combustion Aérothermique Réactivité et Environnement, Centre national de la recherche scientifique (ICARE-CNRS), Orléans, using a number of different reference compounds to determine NO$_3$ reaction rate coefficients for four furans, two furanones, and pyrrole. In the case of the two furanones, this is the first time that NO$_3$ rate coefficients have been reported. The recommended values (cm^3 molec.$^{-1}$ s^{-1}) are as follows: furan, $(1.49 \pm 0.23) \times 10^{-12}$; 2-methylfuran, $(2.26 \pm 0.52) \times 10^{-11}$; 2,5-dimethylfuran, $(1.02 \pm 0.31) \times 10^{-10}$; furfural (furan-2-aldehyde), $(9.07 \pm 2.3) \times 10^{-14}$; α-angelicalactone (5-methyl-2(3H)-furanone), $(3.01 \pm 0.45) \times 10^{-12}$; γ-crotonolactone (2(5H)-furanone), $< 1.4 \times 10^{-16}$; and pyrrole, $(6.94 \pm 1.9) \times 10^{-11}$. The furfural + NO$_3$ reaction rate coefficient is found to be an order of magnitude smaller than previously reported. These experiments show that for furan, alkyl-substituted furans, α-angelicalactone, and pyrrole, reaction with NO$_3$ will be the dominant removal process at night and may also contribute during the day. For γ-crotonolactone, reaction with NO$_3$ is not an important atmospheric sink.

1 Introduction

Furans are five-membered aromatic cyclic ethers. Furans (and pyrroles – where N replaces O as the heteroatom) are generated during the pyrolysis of cellulose and are a major component of emissions from wildfire burning (Hatch et al., 2015, 2017; Koss et al., 2018; Coggon et al., 2019; Andreae, 2019). Such emissions are likely to increase in the future, with the spatial extent, number, and severity of wildfires having increased markedly at the global scale in recent decades (Jolly et al., 2015; Harvey, 2016); this is predicted to continue as the climate warms (Krikken et al., 2021; Lohmander,

2020). Furans have also been measured in emissions from residential logwood burning (Hartikainen et al., 2018) and from the burning of a wide variety of solid fuels used for domestic heating and cooking (Stewart et al., 2021a). Furans have been shown to account for a significant proportion of the total NO$_3$ (Decker et al., 2019) and OH (Koss et al., 2018; Coggon et al., 2019; Stewart et al., 2021b) reactivity of emissions from the burning of typical wildfire and domestic fuels.

Alkyl-substituted furans have also been suggested as promising biofuels, as they can be derived from lignocellulosic biomass (Roman-Leshkov et al., 2007; Binder and Raines, 2009; Wang et al., 2014). This would likely lead to

fugitive emissions of these compounds during distribution as well as to emissions of unburned and partially oxidised products from vehicle exhaust. The oxidation of certain furan compounds has been shown to have large secondary organic aerosol yields (Hatch et al., 2017; Hartikainen et al., 2018; Joo et al., 2019; Ahern et al., 2019; Akherati et al., 2020), which could adversely impact air quality.

Oxidation of furans in the atmosphere has been shown to produce 2-furanones (monounsaturated five-membered cyclic esters) both via OH (notably hydroxy-furan-2-ones; Aschmann et al., 2014) and NO$_3$ (Berndt et al., 1997) reactions. Furan-2-ones are also produced from the OH oxidation of six-membered aromatic compounds (Smith et al., 1998, 1999; Hamilton et al., 2005; Bloss et al., 2005; Wyche et al., 2009; Huang et al., 2014). In both cases, the initial product is thought to be an unsaturated dicarbonyl, with production of the 2-furanone formed via photoisomerisation of the dicarbonyl to a ketene-enol (Newland et al., 2019), followed by ring closure of this molecule. In the case of aromatics, the ketene-enol can also be formed directly via decomposition of the bicyclic peroxy radical intermediate (Wang et al., 2020).

Furan-type compounds are removed from the atmosphere by reaction with the major oxidants OH, NO$_3$, and O$_3$. There have been a number of studies on the rates of reaction of furan-type compounds with the dominant daytime oxidant, OH (Lee and Tang, 1982; Atkinson et al., 1983; Wine and Thompson, 1984; Bierbach et al., 1992, 1994, 1995; Aschmann et al., 2011; Ausmeel et al., 2017; Whelan et al., 2020). However, there have been fewer studies on the rates of reaction of furan-type compounds with the major nighttime oxidant, NO$_3$ (Atkinson et al., 1985; Kind et al., 1996; Cabañas et al., 2004; Colmenar et al., 2012).

The nitrate radical, NO$_3$, is produced in the atmosphere, predominantly through the reaction of NO$_2$ with O$_3$, and exists in equilibrium with N$_2$O$_5$. It has long been known to be an important night-time oxidant (Levy, 1972; Winer et al., 1984). While it is also produced during the daytime, it is rapidly converted back to NO$_2$ by reaction with NO and by photolysis. However, in environments with low NO, either due to low NO$_x$ emissions or suppression through high O$_3$ concentrations (e.g. Newland et al., 2021), NO$_3$ oxidation has been observed to be significant during the day (Hamilton et al., 2021).

Here, we present results of a series of relative rate experiments for furan, 2-methylfuran, 2,5-dimethylfuran, furfural (furan-2-aldehyde), α-angelicalactone (5-methyl-2(3H)-furanone), γ-crotonolactone (2(5H)-furanone), and pyrrole reaction with the NO$_3$ radical, performed in the 7300 L indoor simulation chamber at Institut de Combustion Aérothermique Réactivité et Environnement, Centre national de la recherche scientifique (ICARE-CNRS), Orléans, France.

2 Experimental

2.1 The CSA chamber

The ICARE-CNRS indoor chamber is a 7300 L indoor simulation chamber used for studying reaction kinetics and mechanisms under atmospheric boundary layer conditions. Further details of the chamber set-up and instrumentation are available elsewhere (Zhou et al., 2017). Experiments were performed in the dark at atmospheric pressure (ca. 1000 mbar), with the chamber operated at a slight overpressure to compensate for removal of air for sampling and to prevent ingress of outside air to the chamber. The chamber is in a climate-controlled room, and the temperature was maintained at 299 $\pm$ 2 K.

2.2 Experimental approach

Starting with the chamber filled with clean air, the volatile organic compounds (VOCs) of interest (ca. 3 ppmv) were added, followed by $\sim$ 1 Torr of the inert gas SF$_6$ to monitor the chamber dilution rate. A flow of 5 L min^{-1} of purified air was continuously added throughout the experiment, and air was then removed from the chamber to maintain a constant pressure (this is a slight overpressure to prevent possible ingress of air from outside the chamber). The chamber was left for at least 30 min prior to the start of the experiment to monitor the dilution rate and losses of the VOCs to the chamber walls. These losses, $(1–8) \times 10^{-6}$ s^{-1}, were always smaller than dilution ($\sim 1.2 \times 10^{-5}$ s^{-1}). The reaction was then initiated by continuously introducing an N$_2$O$_5$ sample, held in a trap at $\sim$ 235 K with a part of the purified air flow (2.5–5) L min^{-1} directed through it, for the duration of the experiment. The chamber was monitored until most of the VOC of interest was consumed, with experiments generally taking 0.5–2 h. The experiments were performed under dry conditions (RH $\leq$ 1.5 %).
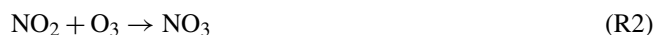
VOC abundance was determined by in situ Fourier transform infrared (FTIR) spectroscopy using a Nicolet 5700 coupled to a White-type multipass cell with a pathlength of 143 m. Each scan was comprised of either 30 or 60 co-additions, taking a total of 2 or 4 min respectively, depending on the expected rate of loss of the VOCs, with a spectral resolution of 0.25 cm^{-1}.

2.3 Materials

The VOCs of interest – furan (>99 %, Sigma-Aldrich), 2-methylfuran (>98 %, TCI), 2,5-dimethylfuran (>98 %, TCI), pyrrole (>99 %, TCI), α-angelicalactone (>98 %, TCI), furfural (>98 %, TCI), and γ-crotonolactone (>93 %, TCI) – and the reference compounds – 2,3-dimethyl-but-2-ene (98 %, Sigma-Aldrich), 2-carene (97 %, Sigma-Aldrich), camphene (95 %, Sigma-Aldrich), α-pinene (98 %, Sigma-Aldrich), cyclohexene ($\geq$99 %, Sigma-Aldrich), 3-methyl-3-buten-1-ol (97 %, Sigma-Aldrich), and cyclohexane (99.5 %,

Sigma-Aldrich) – were used as supplied without further purification.

N$_2$O$_5$ was synthesised by reacting NO$_2$ with excess O$_3$. First, NO and O$_3$ were mixed to generate NO$_2$ (Reaction R1). This NO$_2$/O$_3$ mixture was then flushed into a bulb in which NO$_3$ and subsequently N$_2$O$_5$ were generated through Reactions (R2)–(R3).

$$NO + O_3 \rightarrow NO_2 \tag{R1}$$
$$NO_2 + O_3 \rightarrow NO_3 \tag{R2}$$
$$NO_2 + NO_3 \rightarrow N_2O_5 \tag{R3}$$

N$_2$O$_5$ crystals were then collected in a cold trap at 190 K. The N$_2$O$_5$ sample was purified by trap-to-trap distillation under a flow of O$_2$/O$_3$. The final sample was stored at 190 K and used within a week.

2.4 Analysis

VOC concentrations were monitored by FTIR. The furans generally have a number of major absorption bands in the infrared. The main bands used for analysis are shown in Table 1 (bold) along with other characteristic bands for each compound. Reference spectra of the major bands for each compound taken in the chamber at a resolution of 0.25 cm^{-1} are provided in the Supplement (Figs. S8–S14). The ANIR curve-fitting software (Ródenas, 2018), which implements a least squares fitting algorithm, was used to generate time profiles for each compound based on their reference spectra. Profiles were checked by doing a number of manual subtractions. Example time profiles from an experiment with α-angelicalactone and furan, with cyclohexene as the reference compound, are shown in Fig. 1. Further example plots are provided in the Supplement (Figs. S1–S7). All of the concentration–time profiles are provided in .txt format at https://doi.org/10.5281/zenodo.5721518, and all of the raw FTIR output is provided in .csv format at https://doi.org/10.5281/zenodo.5721518. Relative rate plots for all of the experiments are shown in Fig. 2.

Relative rate experiments were performed, whereby a compound (or two) with an unknown reaction rate coefficient (k_{VOC}) with NO$_3$ was added to the chamber with a reference compound with a known NO$_3$ reaction rate coefficient (k_{ref}). A plot of the relative loss of the compound against the reference compound following addition of NO$_3$ (via N$_2$O$_5$ decomposition), accounting for both chamber dilution and wall losses (k_d), gives a gradient of k_{VOC}/k_{ref} (Eq. 1).

$$\ln\frac{([VOC]_0)}{([VOC]_t)} - k_d t = \frac{k_{VOC}}{k_{ref}} \ln\frac{[ref]_0}{[ref]_t} - k_d t \tag{1}$$

A number of reference compounds were used for each VOC; they were chosen so that the reference rate coefficient was roughly within a factor of 5 of the expected unknown rate coefficient, and an attempt was made to use different referenc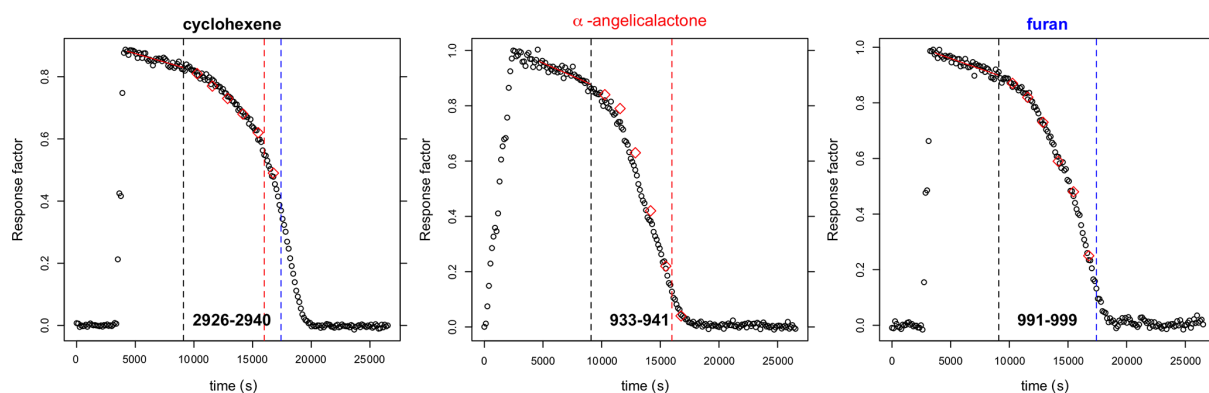es that had both larger and smaller NO$_3$ reaction rate coefficients than the VOC. Rate coefficients of the reference compounds (Table 2) are taken from the Database for the Kinetics of the Gas-Phase Reactions of Organic Compounds v2.1.0 (McGillen et al., 2020), available at https://data.eurochamp.org/data-access/kin/#/home (last access: 27 January 2022).

N$_2$O$_5$ was not present at detectable levels (by FTIR) during most of the experiments. The only experiments in which N$_2$O$_5$ concentrations built up in the chamber were those with the slowest reacting VOCs (i.e. furfural and γ-crotonolactone). NO$_2$ concentrations increased throughout all experiments, typically up to 2–3 ppmv. NO$_2$ is initially produced from the decomposition of N$_2$O$_5$ and, later, potentially by the loss of NO$_2$ from nitrated VOCs/nitrated radicals. HNO$_3$ concentrations increased throughout the experiments, typically up to 3–4 ppmv. This could be caused by either impurities in the N$_2$O$_5$ sample or H-abstraction reactions of NO$_3$. It is not thought that this level of HNO$_3$ will cause any interference in the rate coefficient determinations.

It is noted that no OH scavenger was used in these experiments (as is the case for most, if not all, previous NO$_3$ relative rate studies to the authors' knowledge). NO$_3$ reaction with alkenes tends to proceed by electrophilic addition to the double bond followed by addition of O$_2$ to the resulting radical, leading to a nitrooxy peroxy radical (β-ONO$_2$-RO$_2$) (Barnes et al., 1989; Hjorth et al., 1990). It has recently been shown (Novelli et al., 2021) that there is the possibility of OH formation through the reactions of β-ONO$_2$-RO$_2$ with HO$_2$. HO$_2$ could be generated in these experiments from the abstraction of an H atom by O$_2$ from a β-ONO$_2$-RO radical with available H atoms. The initial NO$_3$ reaction with furans is not thought to form β-ONO$_2$-RO$_2$ radicals, with NO$_3$ addition to the C$_2$ carbon followed by O$_2$ addition to the C$_5$ carbon (Berndt et al., 1997), analogous to the OH-addition reaction (Bierbach et al., 1995; Mousavipour et al., 2009; Yuan et al., 2017; Whelan et al., 2020). However, some of the reference compounds used in the experiments will form such radicals. For example, the reaction of HO$_2$ with the β-ONO$_2$-RO$_2$ radicals formed from α-pinene + NO$_3$ has been reported to have an OH yield of up to 70 % (Kurtén et al., 2017). An additional minor source of HO$_2$ during the experiments will be H-abstraction reactions by NO$_3$. These will produce RO$_2$ that can react to form RO radicals which may yield HO$_2$ following abstraction of an H atom by O$_2$. However, the rate coefficient of H abstraction by NO$_3$ is generally expected to be negligible relative to that of the NO$_3$-addition pathway. A box model run was performed to test the impact of this chemistry in this study. The α-pinene scheme from the Master Chemical Mechanism version v3.3.1 (MCMv3.3.1; Jenkin et al., 1997; http://mcm.york.ac.uk, last access: 27 January 2022) was incorporated into the AtChem box model (Sommariva et al., 2020), and an OH yield of 0.5 was assigned to the reaction of HO$_2$ with the initial β-ONO$_2$-RO$_2$ radicals formed from the α-pinene+NO$_3$ reaction. The model was initiated with

Table 1. Maxima of major absorption bands (of Q branches, if present) for the compounds used in this study. Bands used predominantly for analysis are shown in bold.

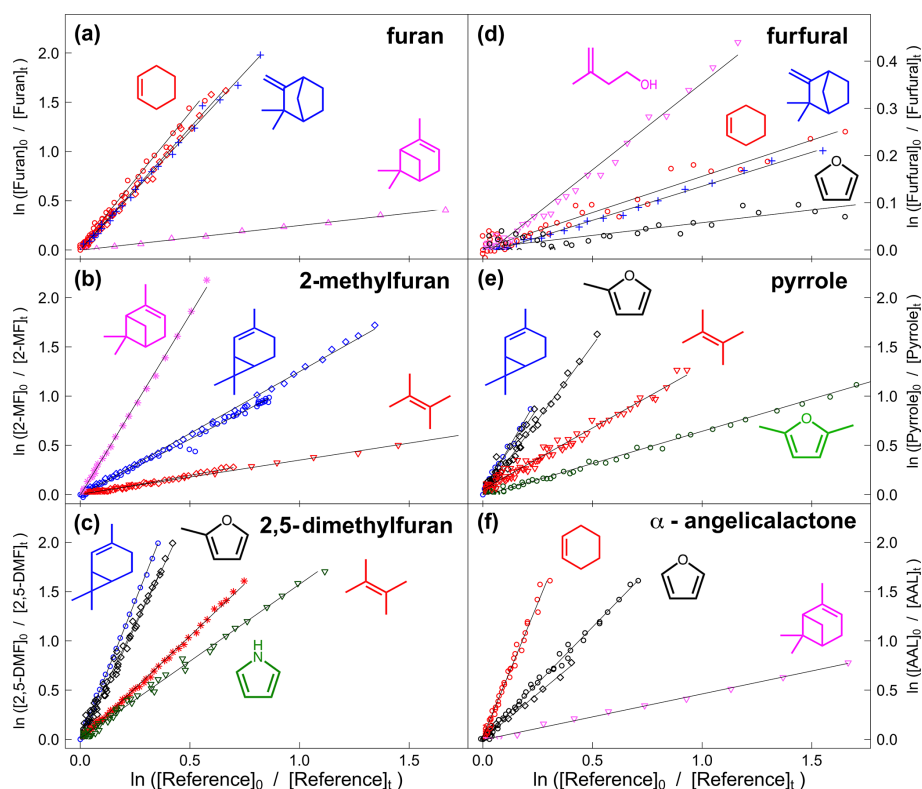| Compound	Main absorption bands (cm^{-1})
furan	**995**, 744
2-methylfuran	**792**, 726, 1151, 2965
2,5-dimethylfuran	**777**, 2938, 2961
furfural	**756**, 1720
pyrrole	**724**, 1017, 3531, 718–722
α-angelicalactone	**731**, **939**, 1100, 1834
γ-crotonolactone	**1098**, 805, 866, 1045, 1812, 2885, 2945
2,3-dimethyl-2-butene	**2878**, **2930**, **3005**
2-carene	**2874**, **2928**, **3009**
α-pinene	**2971**, **2998**, **3035**, 789, 2847, 2893, 2925, 2931
camphene	**2967**, **2972**, **2986**, 882, 2881, 3075
cyclohexene	**2934**, 744, 919, 1140, 2892, 2943, 3033, 3036
3-methyl-3-buten-1-ol	**1065**, 896, 903, 2886, 2948, 2981, 3084
cyclohexane	**2862**, **2933**

Figure 1. Concentration–time profiles from experiment with cyclohexene, α-angelicalactone, and furan. Black circles are response factors generated by the ANIR curve-fitting program relative to the reference spectra. Red diamonds are obtained from manual subtractions. The left black dashed vertical line is the beginning of the region used for the relative rate calculation, the red dashed line is the end of the region used for the calculation of the α-angelicalactone relative rate, and the blue line is the end of the region used for the calculation of the furan relative rate. Bold values at the bottom are the absorption bands used for analysis.

Table 2. Reference compounds used. Recommended rate coefficients and uncertainties from McGillen et al. (2020).

Compound	k (cm^3 molec.$^{-1}$ s^{-1})
2,3-dimethyl-2-butene	$(5.70 \pm 1.71) \times 10^{-11}$
2-carene	$(2.0 \pm 0.3) \times 10^{-11}$
α-pinene	$(6.20 \pm 1.55) \times 10^{-12}$
camphene	$(6.60 \pm 1.65) \times 10^{-13}$
cyclohexene	$(5.60 \pm 0.84) \times 10^{-13}$
3-methyl-3-buten-1-ol	$(2.60 \pm 0.78) \times 10^{-13}$
cyclohexane	$(1.35 \pm 0.20) \times 10^{-16}$

2-methylfuran and α-pinene concentrations of 3 ppmv, representative of the experiments performed here. NO$_3$ concentrations were constrained to give a lifetime of ~ 1 h for the VOCs, typical of the experiments. OH reaction was found to account for less than 1 % of the removal of 2-methylfuran or α-pinene through the model run. Consequently, it can be assumed that OH chemistry is a negligible interference in these experiments.

A further potential interference with the current experimental set-up is the reaction of NO$_2$ with the compounds used. Rate coefficients have been measured for reaction of NO$_2$ with a number of unsaturated compounds (Atkinson et al., 1984b; Bernard et al., 2013). For conjugated dienes, these values can be large enough ($\sim 10^{-18}$ cm^3 molec.$^{-1}$ s^{-1}) to provide a significant loss under the experimental conditions employed here; NO$_2$ is formed during these experiments

Figure 2. Relative rate plots for **(a)** furan relative to cyclohexene (red), camphene (blue), and α-pinene (pink); **(b)** 2-methylfuran relative to 2-carene (blue), 2,3-dimethyl-2-butene (red), and α-pinene (pink); **(c)** 2,5-dimethylfuran relative to 2-carene (blue), 2,3-dimethyl-2-butene (red), 2-methylfuran (black), and pyrrole (green); **(d)** furfural relative to camphene (blue), cyclohexene (red), furan (black), and 3-methyl-3-buten-1-ol (pink); **(e)** pyrrole relative to 2-carene (blue), 2,3-dimethyl-2-butene (red), 2-methylfuran (black), and 2,5-dimethylfuran (green); and **(f)** α-angelicalactone relative to cyclohexene (red), furan (black), and α-pinene (pink). Different shapes are used for different experiments with the same reference compound.

from the decomposition of N$_2$O$_5$, with the NO$_2$ mixing ratio typically increasing up to roughly 3 ppmv through the experiment. Separate experiments were performed to look at the potential reaction of NO$_2$ with furan, 2,5-dimethylfuran, and pyrrole. The experiments were performed with initial VOC mixing ratios of 3 ppmv and initial NO$_2$ mixing ratios of roughly 5 ppmv, similar to the maximum amount of NO$_2$ observed during the NO$_3$ experiments. For all three compounds, their loss in the presence of NO$_2$ (allowing for dilution) was indistinguishable from zero, allowing an upper limit of $<2 \times 10^{-20}$ cm^3 molec.$^{-1}$ s^{-1} to be placed on their $k(\text{NO}_2)$ rate coefficients. Based on these experiments, it was assumed that the $k(\text{NO}_2)$ rate coefficients for 2-methylfuran, furfural, and α-angelicalactone are likely to be of a similar magnitude and, hence, provide negligible interference under the experimental conditions employed.

3 Results and discussion

The $k(\text{NO}_3)$ rate coefficients determined with each reference compound are given in Table 3 and Fig. 3. Overall recommended values for the rate coefficient for each compound are

calculated by taking the mean (weighted by the reported uncertainty of the reference) of the rate coefficient derived from each experiment with each reference compound, including using the recommended values for the other furans presented in Table 3. Uncertainties for the relative rates in Table S1 are assumed to be $<10\,\%$ and to be dominated by statistical errors in fitting to the absorption bands. Uncertainties for the rate coefficients reported in Table 3 are dominated by the assumed uncertainties in $k(\text{NO}_3)$ of the reference compounds. For most of the references, the uncertainties are 20 %–30 %, taken from the recommendations of McGillen et al. (2020). For 2,3-dimethyl-2-butene, the recommended uncertainty in McGillen et al. (2020) is 150 %; however, based on the fact that the rate coefficients derived using 2,3-dimethyl-2-butene for 2-methylfuran, 2,5-dimethylfuran, and pyrrole agree very well with those using other references with much smaller uncertainties, a conservative estimate of 30 % is used here. It is noted that the rate coefficients derived with different references agree very well, to within 10 %, for all compounds. The experimentally determined $k(\text{NO}_3)$ rate coefficients of the furans relative to each other are in good agreement (to within 6 %) with those calculated using the weighted means

shown in Table 3 (Table S2). This gives further confidence in the $k(\text{NO}_3)$ values used for the reference compounds.

The recommended rate coefficients from this work are compared to those previously reported in the literature in Table 4. The rate coefficient derived for furan agrees well with the value previously reported by Atkinson et al. (1985) from a chamber relative rate experiment. However, there is significant differences between the values reported here for furan, 2-methylfuran, and 2,5-dimethylfuran, and those reported by Kind et al. (1996) from relative rate experiments in a flow reactor. While the value reported for 2-methylfuran agrees within the uncertainties between the two studies, the values for furan and 2,5-dimethylfuran reported here are $\sim 50\%$ and 100% greater respectively. It is unclear what is behind this observed disparity; the good agreement between the two studies for the 2-methylfuran rate coefficient suggests that there is not a systematic difference between the experimental set-ups. For pyrrole, the rate coefficient determined here is about 50% faster than the value reported by Atkinson et al. (1985) from a chamber relative rate experiment using N$_2$O$_5$ thermal decomposition. Cabañas et al. (2004) reported an upper limit of $< 1.8 \times 10^{-10}\,\text{cm}^3\,\text{molec.}^{-1}\,\text{s}^{-1}$ (298 K) using an absolute technique of fast flow discharge.

For 2-furanaldehyde (furfural) + NO$_3$, the rate coefficient recommended here is an order of magnitude slower than the only previously reported values (Colmenar et al., 2012), derived from small chamber relative rate experiments with 2-methyl-2-butene and α-pinene as references. The rate coefficient from Colmenar et al. (2012) is very similar to the reported rate coefficient for furan + NO$_3$. This is surprising, as the presence of a formyl group attached to a double bond is expected to be strongly deactivating with respect to addition to that bond, due to the electron withdrawing mesomeric effect of the $-$C(O)H group (Kerdouci et al., 2014). This has also been observed for other electrophilic addition reactions, such as those with OH and O$_3$ (Kwok and Atkinson, 1995; McGillen et al., 2011; Jenkin et al., 2020). Furthermore, while there is the possibility of H abstraction from the formyl group, which would increase the overall rate coefficient, such reactions are typically of the order of $10^{-14}\,\text{cm}^3\,\text{s}^{-1}$ (Kerdouci et al., 2014); hence, they would not be expected to compensate for the reduction in the contribution to the overall rate coefficient of the addition reaction.
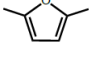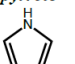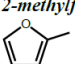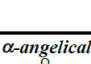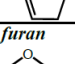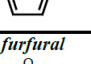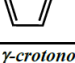
For 5-methyl-(3H)-furan-2-one (α-angelicalactone) + NO$_3$, this is the first reported rate coefficient. For (5H)-furan-2-one (γ-crotonolactone), relative rate experiments with several reference compounds were attempted, with the slowest reacting of these being cyclohexane ($k_{\text{NO}_3} = 1.4 \times 10^{-16}\,\text{cm}^3\,\text{molec.}^{-1}\,\text{s}^{-1}$). In this experiment, roughly 10% of the cyclohexane was removed by reaction with NO$_3$ (accounting for loss by dilution), whereas there was no appreciable chemical loss of γ-crotonolactone. Therefore, we can deduce that $k(\gamma$-crotonolactone + NO$_3$) $\ll 1.4 \times 10^{-16}\,\text{cm}^3\,\text{molec.}^{-1}\,\text{s}^{-1}$. Again, this is the first time a NO$_3$ reaction rate coefficient
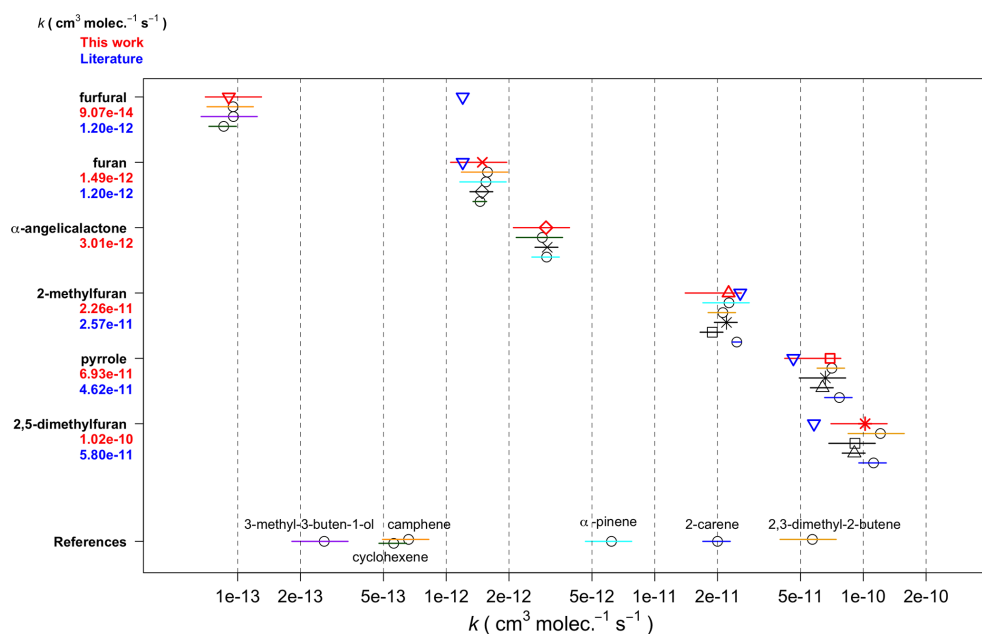
has been measured for this compound. A comparison of the two furanones shows that 5-methyl-(3H)-furan-2-one reacts more than 4 orders of magnitude faster than (5H)-furan-2-one. This can be explained in part by the presence of a methyl group, which is seen to increase the rate coefficient by roughly an order of magnitude from e.g. furan to 2-methylfuran to 2,5-dimethylfuran. Berndt et al. (1997) derived an NO$_3$ reaction rate coefficient of $1.76 \times 10^{-13}\,\text{cm}^3\,\text{molec.}^{-1}\,\text{s}^{-1}$ for (3H)-furan-2-one. However, the majority of the difference must be explained by the structure of the two compounds, namely the conjugated nature of the C$=$C and C$=$O bonds in (5H)-furan-2-one. The carbonyl group removes electron density from the C$=$C bond, greatly reducing the rate coefficient. A similar relationship is seen for analogous acyclic compounds e.g. the NO$_3$ rate coefficient of the conjugated ester methyl acrylate is almost 2 orders of magnitude greater than that of the non-conjugated isomer vinyl acetate.

4 Atmospheric implications

The atmospheric lifetimes of the compounds, based on the rate coefficients reported herein, are given in Table 5. These assume concentrations of OH $= 5 \times 10^6\,\text{molec.}\,\text{cm}^{-3}$ (typical daily peak summertime concentrations of 1.5×10^6–$1.5 \times 10^7\,\text{molec.}\,\text{cm}^{-3}$; Stone et al., 2012), night-time NO$_3 = 2 \times 10^8\,\text{molec.}\,\text{cm}^{-3}$ (typical night-time concentrations of 1×10^8 to $> 1 \times 10^9\,\text{cm}^{-3}$; Brown and Stutz, 2012), daytime NO$_3 = 1 \times 10^7\,\text{molec.}\,\text{cm}^{-3}$ (limited daytime measurements suggest concentrations ~ 0.5 to > 1 pptv, $2.5 \times 10^7\,\text{molec.}\,\text{cm}^{-3}$; Brown and Stutz, 2012), and O$_3 = 40$ ppbv (background O$_3$ concentration ~ 40 ppb; Parrish et al., 2014). It is noted that oxidant concentrations have a high spatial and temporal variability due to variability in their sources and sinks and that oxidant levels within biomass burning plumes in particular are poorly understood. Hence, the relative importance of the oxidants shown in Table 5 is likely to vary depending on conditions. From the values given in Table 5, it is clear that the alkyl-substituted furans and pyrrole have very short lifetimes both during the day, when the dominant daytime sink is likely to be reaction with OH, and at night, when the dominant sink will be reaction with NO$_3$. O$_3$ may contribute somewhat to the removal of these compounds both during the day and night, particularly for 2,5-dimethylfuran. As $k(\text{NO}_3)$ approaches the same order of magnitude as $k(\text{OH})$, e.g. for 2-methylfuran, 2,5-dimethylfuran, and pyrrole, the NO$_3$ reaction is likely to be competitive with the OH reaction even during the day in low-NO$_x$ environments, with daytime NO$_3$ concentrations reported to be ~ 1 ppt ($2.5 \times 10^7\,\text{molec.}\,\text{cm}^{-3}$) (Brown and Stutz, 2012). The relatively large rate coefficient reported here for α-angelicalactone suggests that NO$_3$ reaction will be an important sink for unsaturated non-conjugated cyclic esters. On the other hand, the very small rate coefficient for

Table 3. NO$_3$ reaction rate coefficients derived for each experiment and the recommended value based on the weighted mean.

Compound	Reference (repeats)	k(NO$_3$) (cm^3 molec.$^{-1}$ s^{-1})	Weighted mean k(NO$_3$) (cm^3 molec.$^{-1}$ s^{-1})
2,5-dimethylfuran	2-carene (1)	1.12×10^{-10}	$\mathbf{1.02 \pm 0.31 \times 10^{-10}}$
	2,3-dimethyl-2-butene (1)	1.21×10^{-10}	
	pyrrole (1)	9.12×10^{-11}	
	2-methylfuran (2)	9.06×10^{-11}	
pyrrole	2-carene (1)	7.68×10^{-11}	$\mathbf{6.94 \pm 1.9 \times 10^{-11}}$
	2,3-dimethyl-2-butene (2)	7.07×10^{-11}	
	2,5-dimethylfuran (1)	6.58×10^{-11}	
	2-methylfuran (2)	6.37×10^{-11}	
2-methylfuran	2-carene (3)	2.47×10^{-11}	$\mathbf{2.26 \pm 0.52 \times 10^{-11}}$
	2,3-dimethyl-2-butene (2)	2.12×10^{-11}	
	α-pinene (1)	2.27×10^{-11}	
	pyrrole (2)	1.89×10^{-11}	
	2,5-dimethylfuran (2)	2.21×10^{-11}	
α-angelicalactone	α-pinene (1)	2.89×10^{-12}	$\mathbf{3.01 \pm 0.45 \times 10^{-12}}$
	cyclohexene (1)	3.03×10^{-12}	
	furan (2)	3.05×10^{-12}	
furan	cyclohexene (1)	1.45×10^{-12}	$\mathbf{1.49 \pm 0.23 \times 10^{-12}}$
	α-pinene (1)	1.55×10^{-12}	
	camphene (1)	1.58×10^{-12}	
	α-angelicalactone (2)	1.49×10^{-12}	
furfural	cyclohexene (1)	8.57×10^{-14}	$\mathbf{9.07 \pm 2.30 \times 10^{-14}}$
	3-methyl-3-buten-1-ol (1)	9.54×10^{-14}	
	furan	8.37×10^{-14}	
	camphene (1)	9.50×10^{-14}	
γ-crotonolactone	cyclohexane (1)	$< 1.4 \times 10^{-16}$	$\mathbf{< 1.4 \times 10^{-16}}$

Figure 3. The reaction rate coefficients derived for the six compounds in this work (excluding γ-crotonolactone). Red triangles (and red text, left axis) represent the weighted mean of all experiments in this work, and blue inverted triangles (and blue text, left axis) are the recommended values from McGillen et al. (2020). Horizontal lines represent uncertainty in rate coefficient, and colours (shapes if other furans) represent which reference was used.

Table 4. Recommended NO_3 rate coefficients from this work compared to those reported in the literature. Recommended values from this work (Table 3) are given in bold.

Compound	Rate coefficient (cm³ molec.⁻¹ s⁻¹)	Reference	Technique	NO_3 source
2,5-dimethylfuran	**$(1.02 \pm 0.31) \times 10^{-10}$**	**This work**		
	$(5.78 \pm 0.34) \times 10^{-11}$	Kind et al. (1996)	Flow reactor: relative (*trans*-2-butene)	N_2O_5
pyrrole	**$(6.94 \pm 1.9) \times 10^{-11}$**	**This work**		
	$(4.6 \pm 1.1) \times 10^{-11}$	Atkinson et al. (1985)	Chamber: relative (2-methyl-2-butene)	N_2O_5
	$<1 \times 10^{-10}$	Cabañas et al. (2004)	Flow reactor: absolute (LIF[b] detection of NO_3)	$HNO_3 + F$
2-methylfuran	**$(2.26 \pm 0.52) \times 10^{-11}$**	**This work**		
	$(2.57 \pm 0.17) \times 10^{-11}$	Kind et al. (1996)	Flow reactor: relative (*trans*-2-butene)	N_2O_5
α-angelicalactone	**$(3.01 \pm 0.45) \times 10^{-12}$**	**This work**		
furan	**$(1.49 \pm 0.23) \times 10^{-12}$**	**This work**		
	$(1.5 \pm 0.2) \times 10^{-12}$[a]	Atkinson et al. (1985)	Chamber: relative (*trans*-2-butene)	N_2O_5
	$(0.998 \pm 0.062) \times 10^{-12}$	Kind et al. (1996)	Flow reactor: relative (*trans*-2-butene)	N_2O_5
	$(1.36 \pm 0.8) \times 10^{-12}$	Cabañas et al. (2004)	Flow reactor: absolute (LIF detection of NO_3)	$HNO_3 + F$
furfural	**$(9.07 \pm 2.30) \times 10^{-14}$**	**This work**		
	$(1.17 \pm 0.15) \times 10^{-12}$	Colmenar et al. (2012)	Small chamber: relative (2-methyl-2-butene)	N_2O_5
	$(1.36 \pm 0.38) \times 10^{-12}$	Colmenar et al. (2012)	Small chamber: relative (α-pinene)	N_2O_5
γ-crotonolactone	**$<1.4 \times 10^{-16}$**	**This work**		

[a] Corrected for change to recommended rate for reference (trans-2-butene). [b] LIF represents laser-induced fluorescence.

Table 5. Atmospheric gas-phase lifetimes of the compounds reported herein based on typical midday OH concentrations of 5×10^6 molec. cm⁻³, night-time NO_3 concentrations of 2×10^8 molec. cm⁻³, daytime NO_3 concentrations of 1×10^7 molec. cm⁻³, and background O_3 concentrations of 40 ppbv (1×10^{12} molec. cm⁻³).

Compound	τ_{NO_3} (night)	τ_{NO_3} (day)	τ_{OH} (day)	τ_{O_3}	τ_{total} (day)
2,5-dimethylfuran	0.82 min	16 min	26 min[a]	40 min[b]	8 min
2-methylfuran	3.7 min	74 min	48 min[a]	–	28 min
furan	56 min	19 h	83 min[a]	116 h[c]	77 min
pyrrole	1.2 min	24 min	28 min[d]	18 h[d]	13 min
furfural	15 h	13 d	95 min[e]	–	94 min
α-angelicalactone	28 min	9.3 h	48 min[f]	3.5 h[g]	37 min
γ-crotonolactone	>1.1 year	>22 years	14 h[h]	173 years	14 h

[a] Matsumoto (2011). [b] Dillon et al. (2012). [c] Atkinson et al. (1983). [d] Atkinson et al. (1984a). [e] Bierbach et al. (1995). [f] Bierbach et al. (1994). [g] Estimated (Bierbach et al., 1994). [h] Ausmeel et al. (2017).

the γ-crotonolactone + NO_3 reaction suggests that this will not be an important atmospheric sink. γ-crotonolactone has also been shown to have a very slow reaction with O_3 (lifetime >100 years; Ausmeel et al., 2017), whereas the lifetime is much shorter for reaction with OH, and this will be the predominant gas-phase sink for γ-crotonolactone . Such a slow NO_3 reaction might be expected to extend to all 2-furanones with a conjugated structure, e.g. hydroxyfuranones – major products of OH oxidation of methyl-substituted furans (Aschmann et al., 2014), such that the nitrate reaction may be unimportant in the atmosphere for these structures. However substitution at the double bond is likely to increase the rate coefficient somewhat, as observed for OH and O_3 reactions

with the methyl-substituted form of γ-crotonolactone (Ausmeel et al., 2017).

One of the major sources of furan-type compounds to the atmosphere is wildfires. Wildfire plumes can even be regions of high NO_3 during the day due to suppressed photolysis rates in optically thick plumes (Decker et al., 2021). NO_3 oxidation of furans may be even more important in such plumes than in the background atmosphere. Such plumes can extend over hundreds of kilometres and, hence, affect air quality on a local and regional scale (e.g. Andreae et al., 1988; Brocchi et al., 2018; Johnson et al., 2021). Domestic wood burning is an increasing trend in northern European cities (Chafe et al., 2015). Burning generally occurs in the winter, during which

time (with short daylight hours and peak daytime OH often an order of magnitude lower than during the summer) the reaction with NO_3 is likely to be the dominant fate of furan-type compounds in such emissions, contributing significantly to organic aerosol in urban areas (Kodros et al., 2020).

Berndt et al. (1997) identified the major first-generation products of furan + NO_3 to be the unsaturated dicarbonyl, butenedial, and 2(3H)-furanone, with the NO_3 recycled back to NO_2. However, Tapia et al. (2011) and Joo et al. (2019) found that the major products of the 3-methylfuran + NO_3 reaction predominantly retain the NO_3 functionality. In this case, furan + NO_3 oxidation chemistry may be a significant sink for NO_x, sequestering it in nitrate species; these nitrate species may then release the NO_x far from the source on further gas-phase oxidation or (due to their low volatility) be taken up into aerosol (Joo et al., 2019).

5   Conclusions

Rate coefficients are recommended for reaction of seven furan-type VOCs with NO_3 at 298 K and 760 Torr, based on a series of relative rate experiments. These new recommendations highlight the importance of NO_3 chemistry to the removal of furans and other similar VOCs under atmospheric conditions. The measured rate coefficients suggest that for the three furans reported here, as well as for pyrrole and α-angelicalactone, reaction with NO_3 is likely to be their dominant night-time sink. For the alkyl furans and pyrrole, reaction with NO_3 may also be a significant sink during the daytime. This work also extends the existing database of VOC + NO_3 reactions, providing valuable reference values for future work.

References

Ahern, A. T., Robinson, E. S., Tkacik, D. S., Saleh, R., Hatch, L. E., Barsanti, K. C., Stockwell, C. E., Yokelson, R. J., Presto, A. A., Robinson, A. L., Sullivan, R. C., and Donahue, N. M.: Production of Secondary Organic Aerosol During Aging of Biomass Burning Smoke From Fresh Fuels and Its Relationship to VOC Precursors, J. Geophys. Res.-Atmos., 124, 3583–3606, 2019.

Akherati, A., He, Y., Coggon, M. M., Koss, A. R., Hodshire, A. L., Sekimoto, K., Warneke, C., de Gouw, J., Yee, L., Seinfeld, J. H., Onasch, T. B., Herndon, S. C., Knighton, W. B., Cappa, C. D., Kleeman, M. J., Lim, C. Y., Kroll, J. H., Pierce, J. R., and Jathar, S. H.: Oxygenated Aromatic Compounds are Important Precursors of Secondary Organic Aerosol in Biomass Burning Emissions, Environ. Sci. Technol., 54, 8568–8579, https://doi.org/10.1021/acs.est.0c01345, 2020.

Andreae, M. O.: Emission of trace gases and aerosols from biomass burning – an updated assessment, Atmos. Chem. Phys., 19, 8523–8546, https://doi.org/10.5194/acp-19-8523-2019, 2019.

Andreae, M. O., Browell, E. V., Garstang, M,. Gregory, G. L., Harriss, R. C., Hill, G. F., Jacob, D. J., Pereira, C., Sachse, G. W., Setzer, A. W., Silva Dias, P. L., Talbot, R. W., Torres, A. L., and Wofsy, S. C.: Biomass-burning emissions and associated haze layers over Amazonia, J. Geophys. Res.-Atmos, 93, 1509–1527, 1988.

Aschmann, S. M., Nishino, N., Arey, J., and Atkinson, R.: Kinetics of the Reactions of OH Radicals with 2- and 3-Methylfuran, 2,3- and 2,5-Dimethylfuran, and E- and Z-3-Hexene-2,5-dione, and Products of OH + 2,5-Dimethylfuran, Environ. Sci. Technol., 45, 1859–1865, 2011.

Aschmann, S. M., Nishino, N., Arey J., and Atkinson, R.: Products of the OH radical-initiated reactions of furan, 2- and 3-methylfuran, and 2,3- and 2,5-dimethylfuran in the presence of NO, J. Phys. Chem. A, 118, 457–466, 2014.

Atkinson, R., Aschmann, S. M., and Carter, W. P. L.: Kinetics of the reactions of O$_3$ and OH radicals with furan and thiophene at 298 ± 2 K, Int. J. Chem. Kinet., 15, 51–61, 1983.

Atkinson, R., Aschmann, S. M., Winer, A. M., and Carter, W. P. L.: Rate Constants for the Gas Phase Reactions of OH Radicals and O$_3$ with Pyrrole at 295 ± 1 K and Atmospheric Pressure, Atmos. Environ., 18, 2105–2107, 1984a.

Atkinson, R., Aschmann, S. M., Winer, A. M., and Pitts, J. N.: Gas-phase reactions of NO$_2$ with alkenes and dialkenes, Int. J. Chem. Kinet., 16, 697–706, 1984b.

Atkinson, R., Aschmann, S. M., Winer, A. M., and Carter, W. P. L.: Rate Constants for the Gas Phase Reactions of NO$_3$ Radicals with Furan, Thiophene and Pyrrole at 295 ± 1 K and Atmospheric Pressure, Environ. Sci. Technol., 19, 87–90, 1985.

Ausmeel, S., Andersen, C., Nielsen, O. J., Østerstrøm, F. F., Johnson, M. S., and Nilsson, E. J. K.: Reactions of Three Lactones with Cl, OD, and O$_3$: Atmospheric Impact and Trends in Furan Reactivity, J. Phys. Chem. A, 121, 4123–4131, 2017.

Barnes, I., Bastian, V., Becker, K. H., and Tong, Z.: Kinetics and products of the reactions of nitrate radical with monoalkenes, dialkenes, and monoterpenes, J. Phys. Chem., 94, 2413–2419, 1990.

Bernard, F., Cazaunau, M., Mu, Y., Wang, X., Daële, V., Chen, J., and Mellouki, A.: Reaction of NO$_2$ with conjugated alkenes, J. Phys. Chem. A, 117, 14132–14140, 2013.

Berndt, T., Böge, O., and Rolle, W.: Products of the Gas-Phase Reactions of NO$_3$ Radicals with Furan and Tetramethylfuran, Environ. Sci. Technol., 31, 1157–1162, 1997.

Bierbach, A., Barnes, I., and Becker, K. H.: Rate coefficients for the gas-phase reactions of hydroxyl radicals with furan, 2-methylfuran, 2-ethylfuran and 2,5-dimethylfuran at 300 ± 2 K, Atmos. Environ., 26, 813–817, 1992.

Bierbach, A., Barnes, I., Becker, K. H., and Wiesen, E.: Atmospheric Chemistry of Unsaturated Carbonyls: Butenedial, 4-Oxo-2-pentenal, 3-Hexene-2,5-dione, Maleic Anhydride, 3H-Furan-2-one, and 5-Methyl-3H-furan-2-one, Environ. Sci. Technol., 28, 715–729, 1994.

Bierbach, A., Barnes, I., and Becker, K. H.: Product and kinetic study of the OH-initiated gas-phase oxidation of furan, 2-methylfuran and furanaldehydes at ≈ 300 K, Atmos. Environ., 29, 2651–2660, 1995.

Binder, J. B. and Raines, R. T.: Simple Chemical Transformation of Lignocellulosic Biomass into Furans for Fuels and Chemicals, J. Am. Chem. Soc., 131, 1979–1985, 2009.

Bloss, C., Wagner, V., Jenkin, M. E., Volkamer, R., Bloss, W. J., Lee, J. D., Heard, D. E., Wirtz, K., Martin-Reviejo, M., Rea, G., Wenger, J. C., and Pilling, M. J.: Development of a detailed chemical mechanism (MCMv3.1) for the atmospheric oxidation of aromatic hydrocarbons, Atmos. Chem. Phys., 5, 641–664, https://doi.org/10.5194/acp-5-641-2005, 2005.

Brocchi, V., Krysztofiak, G., Catoire, V., Guth, J., Marécal, V., Zbinden, R., El Amraoui, L., Dulac, F., and Ricaud, P.: Intercontinental transport of biomass burning pollutants over the Mediterranean Basin during the summer 2014 ChArMEx-GLAM airborne campaign, Atmos. Chem. Phys., 18, 6887–6906, https://doi.org/10.5194/acp-18-6887-2018, 2018.

Brown, S. and Stutz, J.: Nighttime radical observations and chemistry, Chem. Soc. Rev., 41, 6405–6447, 2012.

Cabañas, B., Baeza, M. T., Salgado, S., Martín, P., Taccone, R., and Martínez, E.: Oxidation of heterocycles in the atmosphere: Kinetic study of their reactions with NO$_3$ radical, J. Phys. Chem. A, 108, 10818–10823, 2004.

Chafe, Z., Brauer, M., Héroux, M.-E., Klimont, Z., Lanki, T., Salonen, R. O., and Smith, K. R.: Residential heating with wood and coal: health impacts and policy options in Europe and North America, WHO Regional Office for Europe, available at: https://apps.who.int/iris/handle/10665/153671 (last access: 27 January 2022), 2015.

Coggon, M. M., Lim, C. Y., Koss, A. R., Sekimoto, K., Yuan, B., Gilman, J. B., Hagan, D. H., Selimovic, V., Zarzana, K. J., Brown, S. S., Roberts, J. M., Müller, M., Yokelson, R., Wisthaler, A., Krechmer, J. E., Jimenez, J. L., Cappa, C., Kroll, J. H., de Gouw, J., and Warneke, C.: OH chemistry of non-methane organic gases (NMOGs) emitted from laboratory and ambient biomass burning smoke: evaluating the influence of furans and oxygenated aromatics on ozone and secondary NMOG formation, Atmos. Chem. Phys., 19, 14875–14899, https://doi.org/10.5194/acp-19-14875-2019, 2019.

Colmenar, I., Cabañas, B., Martínez, E., Salgado, M. S., and Martín, P.: Atmospheric fate of a series of furanaldehydes by their NO$_3$ reactions, Atmos. Environ., 54, 177–184, 2012.

Decker, Z. C. J., Zarzana, K. J., Coggon, M., Min, K.-E., Pollack, I., Ryerson, T. B., Peischl, J., Edwards, P., Dubeì, W. P., Markovic, M. Z., Roberts, J. M., Veres, P. R., Graus, M., Warneke, C., de Gouw, J., Hatch, L. E., Barsanti, K. C., and Brown, S. S.: Nighttime Chemical Transformation in Biomass Burning Plumes: A Box Model Analysis Initialized with Aircraft Observations, Environ. Sci. Technol., 53, 2529–2538, https://doi.org/10.1021/acs.est.8b05359, 2019.

Decker, Z. C. J., Robinson, M. A., Barsanti, K. C., Bourgeois, I., Coggon, M. M., DiGangi, J. P., Diskin, G. S., Flocke, F. M., Franchin, A., Fredrickson, C. D., Gkatzelis, G. I., Hall, S. R., Halliday, H., Holmes, C. D., Huey, L. G., Lee, Y. R., Lindaas, J., Middlebrook, A. M., Montzka, D. D., Moore, R., Neuman, J. A., Nowak, J. B., Palm, B. B., Peischl, J., Piel, F., Rickly, P. S., Rollins, A. W., Ryerson, T. B., Schwantes, R. H., Sekimoto, K., Thornhill, L., Thornton, J. A., Tyndall, G. S., Ullmann, K., Van Rooy, P., Veres, P. R., Warneke, C., Washenfelder, R. A., Weinheimer, A. J., Wiggins, E., Winstead, E., Wisthaler, A., Womack, C., and Brown, S. S.: Nighttime and daytime dark oxidation chemistry in wildfire plumes: an observation and model analysis of FIREX-AQ aircraft data, Atmos. Chem. Phys., 21, 16293–16317, https://doi.org/10.5194/acp-21-16293-2021, 2021.

Dillon, T. J., Tucceri, M. E., Dulitz, K., Horowitz, A., Vereecken, L., and Crowley, J.: Reaction of Hydroxyl Radicals with C$_4$H$_5$N (Pyrrole): Temperature and Pressure Dependent Rate Coefficients, J. Phys. Chem. A, 116, 6051–6058, 2012.

Hamilton, J. F., Webb, P. J., Lewis, A. C., and Reviejo, M. M.: Quantifying small molecules in secondary organic aerosol formed during the photo-oxidation of toluene with hydroxyl radicals, Atmos. Environ., 39, 7263–7275, 2005.

Hamilton, J. F., Bryant, D. J., Edwards, P. E., Quyang, B., Bannan, T. J., Mehra, A., Mayhew, A. W., Hopkins, J. R., Dunmore, R. E.,

Squires, F. A., Lee, J. D., Newland, M. J., Worrall, S. D., Bacak, A., Coe, H., Percival, C., Whalley, L. K., Heard, D. E., Slater, E. J., Jones, R. L., Cui, T., Surratt, J. D., Reeves, C. E., Mills, G. P., Grimmond, S., Sun, Y., Xu, W., Shi, Z., and Rickard, A. R.: Key Role of NO$_3$ Radicals in the Production of Isoprene Nitrates and Nitrooxyorganosulfates in Beijing, Environ. Sci. Technol., 55, 842–853, https://doi.org/10.1021/acs.est.0c05689, 2021.

Hartikainen, A., Yli-Pirilä, P., Tiitta, P., Leskinen, A., Kortelainen, M., Orasche, J., Schnelle-Kreis, J., Lehtinen, K., Zimmermann, R., Jokiniemi, J., and Sippula, O.: Volatile Organic Compounds from Logwood Combustion: Emissions and Transformation under Dark and Photochemical Aging Conditions in a Smog Chamber, Environ. Sci. Technol., 52, 4979–4988, 2018.

Harvey B. J.: Human-caused climate change is now a key driver of forest fire activity in the western United States, P. Natl. Acad. Sci. USA, 113, 11649–11650, 2016.

Hatch, L. E., Luo, W., Pankow, J. F., Yokelson, R. J., Stockwell, C. E., and Barsanti, K. C.: Identification and quantification of gaseous organic compounds emitted from biomass burning using two-dimensional gas chromatography–time-of-flight mass spectrometry, Atmos. Chem. Phys., 15, 1865–1899, https://doi.org/10.5194/acp-15-1865-2015, 2015.

Hatch, L. E., Yokelson, R. J., Stockwell, C. E., Veres, P. R., Simpson, I. J., Blake, D. R., Orlando, J. J., and Barsanti, K. C.: Multi-instrument comparison and compilation of non-methane organic gas emissions from biomass burning and implications for smoke-derived secondary organic aerosol precursors, Atmos. Chem. Phys., 17, 1471–1489, https://doi.org/10.5194/acp-17-1471-2017, 2017.

Hjorth, J., Lohse, C., Nielsen, C. J., Skov, H., and Restelli, G.: Products and mechanism of the gas-phase reaction between NO$_3$ and a series of alkenes, J. Phys. Chem., 94, 7494–7500, 1990.

Huang, M. Q., Hu, C. J., Guo, X. Y., Gu, X. J., Zhao, W. X., Wang, Z. Y., Fang ,L., and Zhang, W. J.: Chemical composition of gas and particle-phase products of OH-initiated oxidation of 1,3,5-trimethylbenzene, Atmos. Pollut. Res., 5, 73–78, 2014.

Jenkin, M. E., Saunders, S. M., and Pilling, M. J.: The tropospheric degradation of volatile organic compounds: a protocol for mechanism development, Atmos. Environ., 31, 81–104, https://doi.org/10.1016/S1352-2310(96)00105-7, 1997 (data available at: http://mcm.york.ac.uk, last access: 27 January 2022).

Jenkin, M. E., Valorso, R., Aumont, B., Newland, M. J., and Rickard, A. R.: Estimation of rate coefficients for the reactions of O$_3$ with unsaturated organic compounds for use in automated mechanism construction, Atmos. Chem. Phys., 20, 12921–12937, https://doi.org/10.5194/acp-20-12921-2020, 2020.

Johnson, M. S., Strawbridge, K., Knowland, K. E., Keller, C., and Travis, M.: Long-range transport of Siberian biomass burning emissions to North America during FIREX-AQ, Atmos. Environ., 252, 118241, https://doi.org/10.1016/j.atmosenv.2021.118241, 2021.

Jolly, W. M., Cochrane, M. A., Freeborn, P. H., Holden, Z. A., Brown, T. J., Williamson, G. J., and Bowman, D. M. J. S.: Climate-induced variations in global wildfire danger from 1979 to 2013, Nat. Commun., 6, 7537, https://doi.org/10.1038/ncomms8537, 2015.

Joo, T., Rivera-Rios, J. C., Takeuchi, M., Alvarado, M. J., and Ng, N. L.: Secondary Organic Aerosol Formation from Reaction of 3-Methylfuran with Nitrate Radicals, ACS Earth Space Chem. 3, 922–934, 2019.

Kerdouci, J., Picquet-Varrault, B., and Doussin, J.-F.: Structure activity relationship for the gas-phase reactions of NO$_3$ radical with organic compounds: Update and extension to aldehydes, Atmos. Environ., 84, 363–372, 2014.

Kind, I., Berndt, T., Böge, O., and Rolle, W.: Gas-phase rate constants for the reaction of NO$_3$ radicals with furan and methyl-substituted furans, Chem. Phys. Lett., 256, 679–683, 1996.

Kodros, J., Papanastasiou, D., Paglione, M., Masiol, M., and Squizzato, S.: Rapid dark aging of biomass burning as an overlooked source of oxidized organic aerosol, P. Natl. Acad. Sci. USA, 117, 33028–33033, 2020.

Koss, A. R., Sekimoto, K., Gilman, J. B., Selimovic, V., Coggon, M. M., Zarzana, K. J., Yuan, B., Lerner, B. M., Brown, S. S., Jimenez, J. L., Krechmer, J., Roberts, J. M., Warneke, C., Yokelson, R. J., and de Gouw, J.: Non-methane organic gas emissions from biomass burning: identification, quantification, and emission factors from PTR-ToF during the FIREX 2016 laboratory experiment, Atmos. Chem. Phys., 18, 3299–3319, https://doi.org/10.5194/acp-18-3299-2018, 2018.

Krikken, F., Lehner, F., Haustein, K., Drobyshev, I., and van Oldenborgh, G. J.: Attribution of the role of climate change in the forest fires in Sweden 2018, Nat. Hazards Earth Syst. Sci., 21, 2169–2179, https://doi.org/10.5194/nhess-21-2169-2021, 2021.

Kurtén, T., Møller, K. H., Nguyen, T. B., Schwantes, R. H., Misztal, P. K., Su, L., Wennberg, P. O., Fry J. L., and Kjaergaard, H. G.: Alkoxy Radical Bond Scissions Explain the Anomalously Low Secondary Organic Aerosol and Organonitrate Yields From alpha-Pinene + NO$_3$, J. Phys. Chem. Lett., 8, 2826–2834, 2017.

Kwok, E. S. C. and Atkinson, R.: Estimation of hydroxyl radical reaction rate constants for gas-phase organic compounds using a structure-reactivity relationship: An update, Atmos. Environ., 29, 1685–1695, https://doi.org/10.1016/1352-2310(95)00069-b, 1995.

Lee, J. H. and Tang, I. N.: Absolute rate constants for the hydroxyl radical reactions with ethane, furan, and thiophene at room temperature, J. Chem. Phys., 77, 4459–4463, 1982.

Levy, H.: Photochemistry of the lower troposphere, Planet Space Sci., 20, 919–935, 1972.

Lohmander, P.: Forest fire expansion under global warming conditions: Multivariate estimation, function properties, and predictions for 29 countries, Central Asian Journal of Environmental Science and Technology Innovation, 5, 262–276, 2020.

Matsumoto, J.: Kinetics of the reactions of ozone with 2,5-dimethylfuran and its atmospheric implications, Chem. Lett., 40, 582–583, 2011.

McGillen, M. R., Archibald, A. T., Carey, T., Leather, K. E., Shallcross, D. E., Wenger, J. C., and Percival, C. J.: Structure-activity relationship (SAR) for the prediction of gas-phase ozonolysis rate coefficients: an extension towards heteroatomic unsaturated species, Phys. Chem. Chem. Phys., 13, 2842–2849, 2011.

McGillen, M. R., Carter, W. P. L., Mellouki, A., Orlando, J. J., Picquet-Varrault, B., and Wallington, T. J.: Database for the kinetics of the gas-phase atmospheric reactions of organic compounds, Earth Syst. Sci. Data, 12, 1203–1216, https://doi.org/10.5194/essd-12-1203-2020, 2020.

Mousavipour, S. H., Ramadan, S., and Shahkolahi, Z: Multichannel RRKM-TST and Direct-Dynamics VTST Study of the Reaction

of Hydroxyl Radical with Furan, J. Phys., Chem., 113, 2838–2846, 2009.

Newland, M.: Experimental datasets from Newland et al. (2021, ACP, NO$_3$ chemistry of wildfire emissions: a kinetic study of the gas-phase reactions of furans with the NO$_3$ radical), Zenodo [data set], https://doi.org/10.5281/zenodo.5724967, 2021a.

Newland, M.: Experimental datasets from Newland et al. (2021, ACP, NO$_3$ chemistry of wildfire emissions: a kinetic study of the gas-phase reactions of furans with the NO$_3$ radical), Zenodo [data set], https://doi.org/10.5281/zenodo.5721518, 2021b.

Newland, M. J., Rea, G. J., Thüner, L. P., Henderson, A. P., Golding, B. T., Rickard, A. R., Barnes, I., and Wenger, J.: Photochemistry of 2-butenedial and 4-oxo-2-pentenal under atmospheric boundary layer conditions, Phys. Chem. Chem. Phys., 21, 1160–1171, 2019.

Newland, M. J., Bryant, D. J., Dunmore, R. E., Bannan, T. J., Acton, W. J. F., Langford, B., Hopkins, J. R., Squires, F. A., Dixon, W., Drysdale, W. S., Ivatt, P. D., Evans, M. J., Edwards, P. M., Whalley, L. K., Heard, D. E., Slater, E. J., Woodward-Massey, R., Ye, C., Mehra, A., Worrall, S. D., Bacak, A., Coe, H., Percival, C. J., Hewitt, C. N., Lee, J. D., Cui, T., Surratt, J. D., Wang, X., Lewis, A. C., Rickard, A. R., and Hamilton, J. F.: Low-NO atmospheric oxidation pathways in a polluted megacity, Atmos. Chem. Phys., 21, 1613–1625, https://doi.org/10.5194/acp-21-1613-2021, 2021.

Novelli, A., Cho, C., Fuchs, H., Hofzumahaus, A., Rohrer, F., Tillmann, R., Kiendler-Scharr, A., Wahner, A., and Vereecken, L.: Experimental and theoretical study on the impact of a nitrate group on the chemistry of alkoxy radicals, Phys. Chem. Chem. Phys., 23, 5474–5495, 2021.

Parrish, D. D., Lamarque, J. F., Naik, V., Horowitz, L., Shindell, D. T., Staehelin, J., Derwent, R., Cooper, O. R., Tanimoto, H., Volz-Thomas, A., Gilge, S., Scheel, H. E., Steinbacher, M., and Fröhlich, M.: Long-term changes in lower tropospheric baseline ozone concentrations: Comparing chemistry-climate models and observations at northern midlatitudes, J. Geophys. Res., 119, 5719–5736, https://doi.org/10.1002/2013JD021435, 2014.

Ródenas, M: Software for analysis of Infrared spectra, EUROCHAMP-2020 project, available at: https://data.eurochamp.org/anasoft (last access: 27 January 2022), 2018.

Roman-Leshkov, Y., Barrett, C. J., Liu, Z. Y., and Dumesic, J. A.: Production of Dimethylfuran for Liquid Fuels from Biomass-derived Carbohydrates, Nature, 447, 982–985, 2007.

Smith, D. F., McIver, C. D., and Kleindienst, T. E.: Primary product distribution from the reaction of hydroxyl radicals with toluene at ppb NO$_x$ mixing ratios, J. Atmos. Chem., 30, 209–228, 1998.

Smith, D. F., Kleindienst, T. E., and McIver, C. D.: Primary Product Distributions from the Reaction of OH with m-, p-Xylene, 1,2,4- and 1,3,5-Trimethylbenzene, J. Atmos. Chem., 34, 339–364, 1999.

Sommariva, R., Cox, S., Martin, C., Borońska, K., Young, J., Jimack, P. K., Pilling, M. J., Matthaios, V. N., Nelson, B. S., Newland, M. J., Panagi, M., Bloss, W. J., Monks, P. S., and Rickard, A. R.: AtChem (version 1), an open-source box model for the Master Chemical Mechanism, Geosci. Model Dev., 13, 169–183, https://doi.org/10.5194/gmd-13-169-2020, 2020.

Stewart, G. J., Acton, W. J. F., Nelson, B. S., Vaughan, A. R., Hopkins, J. R., Arya, R., Mondal, A., Jangirh, R., Ahlawat, S., Yadav, L., Sharma, S. K., Dunmore, R. E., Yunus, S. S. M., Hewitt, C. N., Nemitz, E., Mullinger, N., Gadi, R., Sahu, L. K., Tripathi, N., Rickard, A. R., Lee, J. D., Mandal, T. K., and Hamilton, J. F.: Emissions of non-methane volatile organic compounds from combustion of domestic fuels in Delhi, India, Atmos. Chem. Phys., 21, 2383–2406, https://doi.org/10.5194/acp-21-2383-2021, 2021a.

Stewart, G. J., Nelson, B. S., Acton, W. J. F., Vaughan, A. R., Hopkins, J. R., Yunus, S. S. M., Hewitt, C. N., Nemitz, E., Mullinger, N., Gadi, R., Rickard, A. R., Lee, J. D., Mandal, T. K., and Hamilton, J. F.: Comprehensive organic emission profiles, secondary organic aerosol production potential, and OH reactivity of domestic fuel combustion in Delhi, India, Environ. Sci. Atmos., 1, 104–117, https://doi.org/10.1039/D0EA00009D, 2021b.

Stone, D., Whalley, L., and Heard, D.: Tropospheric OH and HO$_2$ radicals: field measurements and model comparisons, Chem. Soc. Rev., 41, 6348–6404, 2012.

Tapia, A., Villanueva, F., Salgado, M. S., Cabañas, B., Martínez, E., and Martín, P.: Atmospheric degradation of 3-methylfuran: kinetic and products study, Atmos. Chem. Phys., 11, 3227–3241, https://doi.org/10.5194/acp-11-3227-2011, 2011.

Wang, J. J., Liu, X. H., Hu, B. C., Lu, G. Z., and Wang, Y. Q.: Efficient Catalytic Conversion of Lignocellulosic Biomass into Renewable Liquid Biofuels via Furan Derivatives, RSC Adv., 4, 31101–31107, 2014.

Wang, S., Newland, M. J., Deng, W., Rickard, A. R., Hamilton, J. F., Muñoz, A., Ródenas, M., Vázquez, M. M., Wang, L., and Wang, X.: Aromatic Photo-oxidation, A New Source of Atmospheric Acidity, Environ. Sci. Technol., 54, 7798–7806, https://doi.org/10.1021/acs.est.0c00526, 2020.

Whelan, C. A., Eble, J. Mir, Z. S., Blitz, M. A., Seakins, P. W., Olzmann, M., and Stone D.: Kinetics of the Reactions of Hydroxyl Radicals with Furan and Its Alkylated Derivatives 2-Methyl Furan and 2,5-Dimethyl Furan, J. Phys. Chem. A, 124, 7416–7426, 2020.

Wine, P. H. and Thompson, R. J.: Kinetics of OH reactions with furan, thiophene, and tetrahydrothiophene, Int. J. Chem. Kinet., 16, 867–878, 1984.

Winer, A. M., Atkinson, R., and Pitts, J. N.: Gaseous Nitrate Radical: Possible Nighttime Atmospheric Sink for Biogenic Organic Compounds, Science, 224, 156–159, 1984.

Wyche, K. P., Monks, P. S., Ellis, A. M., Cordell, R. L., Parker, A. E., Whyte, C., Metzger, A., Dommen, J., Duplissy, J., Prevot, A. S. H., Baltensperger, U., Rickard, A. R., and Wulfert, F.: Gas phase precursors to anthropogenic secondary organic aerosol: detailed observations of 1,3,5-trimethylbenzene photooxidation, Atmos. Chem. Phys., 9, 635–665, https://doi.org/10.5194/acp-9-635-2009, 2009.

Yuan, Y., Zhao, X., Wang, S., and Wang, L: Atmospheric Oxidation of Furan and Methyl-Substituted Furans Initiated by Hydroxyl Radicals, J. Phys. Chem. A, 121, 9306–9319, 2017.

Zhou, L., Ravishankara, A. R., Brown, S. S., Idir, M., Zarzana, K. J., Daële, V., and Mellouki, A.: Kinetics of the Reactions of NO$_3$ Radical with Methacrylate Esters, J. Phys. Chem. A, 121, 4464–4474, 2017.